Effective gene therapy in an authentic model of Tay-Sachs-related diseases

M. Begoña Cachón-González*, Susan Z. Wang*, Andrew Lynch†, Robin Ziegler‡, Seng H. Cheng‡, and Timothy M. Cox*§

*Department of Medicine, University of Cambridge, Level 5, Box 157, Addenbrooke's Hospital, Hills Road, Cambridge CB2 2QQ, United Kingdom; †Centre for Applied Medical Statistics, Department of Public Health and Primary Care, University Forvie Site, Robinson Way, Cambridge CB2 2SR, United Kingdom; and ‡Genzyme Corporation, 31 New York Avenue, Framingham, MA 01701-9322

Communicated by Douglas T. Fearon, University of Cambridge, Cambridge, United Kingdom, May 11, 2006 (received for review March 23, 2006)

Tay-Sachs disease is a prototypic neurodegenerative disease. Lysosomal storage of GM2 ganglioside in Tay-Sachs and the related disorder, Sandhoff disease, is caused by deficiency of β-hexosaminidase A, a heterodimeric protein. Tay-Sachs-related diseases (GM2 gangliosidoses) are incurable, but gene therapy has the potential for widespread correction of the underlying lysosomal defect by means of the secretion-recapture cellular pathway for enzymatic complementation. Sandhoff mice, lacking the β-subunit of hexosaminidase, manifest many signs of classical human Tay-Sachs disease and, with an acute course, die before 20 weeks of age. We treated Sandhoff mice by stereotaxic intracranial inoculation of recombinant adeno-associated viral vectors encoding the complementing human β-hexosaminidase α and β subunit genes and elements, including an HIV tat sequence, to enhance protein expression and distribution. Animals survived for >1 year with sustained, widespread, and abundant enzyme delivery in the nervous system. Onset of the disease was delayed with preservation of motor function; inflammation and GM2 ganglioside storage in the brain and spinal cord was reduced. Gene delivery of β-hexosaminidase A by using adeno-associated viral vectors has realistic potential for treating the human Tay-Sachs-related diseases.

adeno-associated virus | GM2 gangliosidosis | neurodegeneration

Hydrolysis of GM2 ganglioside in the lysosome is catalyzed by β-hexosaminidase (Hex) A and requires the cofactor, GM2 activator protein. Inborn errors with defective breakdown of GM2 ganglioside and cognate gangliosides cause pathological storage principally in the nervous system and are associated with severe neurodegeneration in Tay-Sachs and related diseases (GM2 gangliosidosis) (1–3).

Hex A is a heterodimer of α and β subunits encoded by the human HEXA and HEXB genes, respectively. Classical infantile (acute) forms of Hex A deficiency (Tay-Sachs), GM2 activator and combined deficiency of Hex A, and the β homodimer, Hex B (Sandhoff disease), are associated with motor weakness, blindness, decerebrate rigidity, and death by 2–5 years of age; attenuated, juvenile, and chronic adult forms also occur. Clinically, these Tay-Sachs-related diseases are almost indistinguishable, but their onset appears to be determined by residual hexosaminidase function. Distended neurones with membranous cytoplasmic bodies due to intralysosomal ganglioside are conspicuous; in the terminal stages, neuronal loss, gliosis, and storage occurs throughout the nervous system.

Mice lacking Hex A and B activity as a result of targeted disruption of the hex β subunit gene (Sandhoff strain) provide an authentic model of acute human Tay-Sachs disease and are invaluable for evaluation of innovative therapies (4, 5). Indistinguishable from wild-type and heterozygous littermates at birth, homozygous hexb −/− mice grow normally to early adulthood. Neurological impairment is apparent at 3 months with head tremor, followed by ataxia, bradykinesia, impaired power, and balance. By 4.5 months, hind-limb movement is lost; Sandhoff mice die before the age of 5 months (Movie 1, which is published as supporting information on the PNAS web site).

The molecular pathogenesis of brain injury associated with GM2 storage in humans and animals is ill understood. Disruption of intracellular structures by the expanded lysosomal compartment, enhanced excitatory neurotransmitter activity with abnormal neurite outgrowth (6), and the accumulation of cytotoxic metabolites (7) may all contribute. Impaired generation of isoglobotrihexosylceramide in Sandhoff mice causes depletion of natural killer T (NKT) cells, a distinct lineage of T cells, indicating that presentation of lysosomal ligands is defective, thereby altering NKT cell responses to infection, malignancy, and immune recognition (8).

Burgeoning evidence links inflammatory responses involving microglia and bone marrow-derived macrophages to neurological injury in GM2 gangliosidoses, and progression of inflammatory changes and brain injury is retarded in Sandhoff mice crossbred onto a strain lacking macrophage inhibitory protein 1-α (9–11).

With widespread inflammation and storage of GM2 and other gangliosides, the Tay-Sachs-related diseases present formidable challenges for treatment. Although allogeneic bone marrow transplantation has little benefit in human GM2 gangliosidosis, it partially repopulates the nervous system with healthy donor macrophages and ameliorates disease in the Sandhoff mouse (9). The use of inhibitors of glycosphingolipid synthesis to balance formation with the impaired catabolism also delays the onset of neurological signs in Sandhoff mice (5). However, in the absence of appreciable hexosaminidase activity in this knockout strain or in the acute human GM2 gangliosidoses, monotherapy with substrate-reducing agents will not arrest the disease.

Here we report the use of gene therapy delivered directly to the brain for murine GM2 gangliosidosis. Adult Sandhoff mice were stereotaxically inoculated with recombinant adeno-associated viral (rAAV) vectors encoding complementing human β-hexosaminidase α and β subunits (rAAVα and rAAVβ). Widespread and sustained expression of hexosaminidase activity in the brain and spinal cord reduced pathological storage and inflammation. When onset of neurological signs was delayed markedly and the pattern of disability was attenuated, survival was greatly prolonged.

Results

A Single Striatal Injection Restores β-Hexosaminidase Activity. Sandhoff mice or those receiving rAAV2/2α as vector control, showed no β-hexosaminidase activity in brain and spinal cord, but after a single striatal injection of rAAV2/2α+β or rAAV2/2β alone at four weeks, widespread activity staining was observed (Fig. 1).

Bilateral distribution of enzyme activity was observed in transduced Sandhoff mice. Maximal activity, showing an intense red

Conflict of interest statement: No conflicts declared.

Freely available online through the PNAS open access option.

Abbreviations: AAV, adeno-associated virus; PAS, periodic acid/Schiff; rAAV, recombinant adeno-associated virus.

§To whom correspondence should be addressed. E-mail: tmc12@medschl.cam.ac.uk.

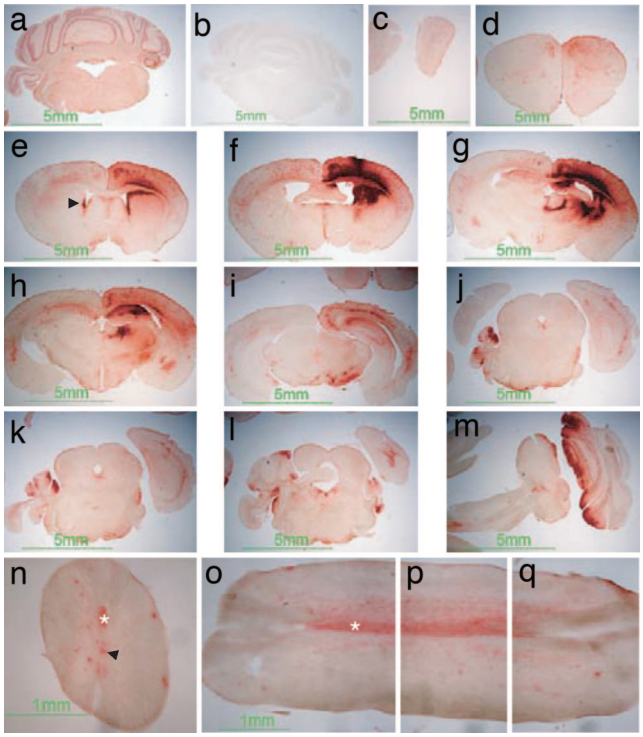

Fig. 1. β-hexosaminidase activity in murine brain and spinal cord after gene therapy. Red staining indicates β-hexosaminidase product in wild-type control (*a*) and in rAAV2/2β-transduced Sandhoff mice (*c–q*), absent in untreated Sandhoff mice (*b*). rAAV2/2β was stereotaxically inoculated at a single site in the right striatum at 4 weeks and killed at the humane end point of 35 weeks of age. Staining extends from the olfactory bulbs (*c*) to the spinal cord (*n–q*). Staining is also observed in ependymal cells in lateral ventricles and the central canal of the spinal cord (arrowheads in *e* and *n*, respectively) and in white matter, particularly evident in the pyramidal tract (asterisk in n–*q*). Reconstruction of a single longitudinal section of spinal cord is depicted in *o–q*. Sections *c–q* were obtained from the animal shown in Movie 2, which is published as supporting information on the PNAS web site.

product, occurred in the vicinity of the injection track. β-Hexosaminidase activities in this area greatly exceeded those in the wild-type brain, which showed homogeneous but less intense staining. Enzymatic activity was widely distributed and extended rostrally to the olfactory bulbs and caudally as far as the spinal cord. β-Hexosaminidase staining was seen in neuronal cell bodies and axonal tracts, the latter most evident in the spinal cord (Fig. 1 *n–q*). The pyramidal tract and spinal gray matter contralateral to the injection site showed the strongest staining, mapping to the decussation of pyramidal tracts (Fig. 1 *n–q*). Prominent enzymatic staining occurred in ependyma lining the ventricles (Fig. 1*e*) and the entire central canal of the spinal cord (Fig. 1*n*).

Enzyme expression was sustained: No difference in the distribution or staining intensity was observed between animals analyzed after 3 or 30 weeks after injection. Similar results were obtained with the AAV2/1 serotype vector (data not shown).

Hexosaminidase Expression Induced by Vector Harboring the β-Subunit Alone. To investigate the ability to restore functional isoforms, enzymatic activities were determined fluorimetrically in the right and left cerebral hemispheres and liver from wild-type, untransduced Sandhoff mice, or those transduced with vectors expressing the α, β, or both enzyme subunits, at a single striatal site (12). As judged by heat inactivation, in wild-type brain, 83% of total β-hexosaminidase was due to Hex A isozyme. Total β-hexosaminidase in untransduced and rAAV2/2α-transduced Sandhoff brain and liver extracts was ≈0.5% and <7% that of respective wild-type activities. In the ipsilateral hemisphere of rAAV2/2β-transduced mice, mean total hexosaminidase was 15-fold greater than wild type, and isozyme analysis indicated 95% Hex A. In the contralateral hemisphere, mean activity was restored to 54% of wild type, 80% of which was attributed to thermolabile Hex A; total hepatic β-hexosaminidase was unchanged at 2% of wild type. Cerebral Hex B activity in transduced animals was increased 5-fold ipsilaterally and restored to a mean of 64% of wild-type activity in the brain, contralaterally. In animals cotransduced with both α and β subunit genes, the proportion of hexosaminidase apparently due to the A isozyme was similar to that induced by administration of the β subunit gene alone (Table 1, which is published as supporting information on the PNAS web site).

β-Hexosaminidase Delivery Prevents Glycosphingolipid Storage and Inflammation. In all parts of the brain, including olfactory bulbs, brainstem, and spinal cord in Sandhoff mice receiving a single striatal injection of vectors harboring α and β, or only β subunits, at the age of 4 weeks, GM2 and GA2 ganglioside storage was reduced compared with untreated 16-week-old animals. Clearance was most evident in the ipsilateral cerebral hemisphere, but G_{M2} and G_{A2} storage continued after single injections of vector; similar effects were observed with each type of injection (Fig. 2 *A* and *B*). Multiple injections of vector led to greater reduction of ganglioside storage, which persisted over the lifetime of Sandhoff mice (Fig. 5, which is published as supporting information on the PNAS web site).

Electron-dense membranous vesicles persisted in cerebral neurones contralateral to the injection site; these vesicles were absent in corresponding neurones from the ipsilateral cortex in an animal killed at 16 weeks of age and after a single striatal inoculation of rAAV2/2α+β (Fig. 2*C*).

The relationship between transgene expression, glycosphingolipid storage and inflammation was examined in consecutive sections of brain and spinal cord from Sandhoff mice transduced with rAAV2/2α+β or rAAV2/2β alone. The number of storage cells staining with periodic acid/Schiff (PAS) reagent and the *Griffonia simplicifolia* isolectin B_4 ($GSIB_4$) and CD68 microglia/macrophage markers varied inversely with the activity of β-hexosaminidase (Fig. 3). Modest expression of hexosaminidase was sufficient to reduce the number of cells expressing microglia/macrophage antigens, even though florid ganglioside storage, shown by PAS, persisted in many cells. Similar results were obtained with each vector.

Rescue of Neurological Function, Improved Survival, and Maintenance of Body Weight. There was no evident difference between rAAV2/2α-treated and untreated Sandhoff mice with respect to onset and progression of symptoms or survival to the humane endpoint. However, a single striatal injection of rAAV2/2α+β was sufficient to increase the disease-free interval by nearly 90%; the mean time to reach the endpoint by animals receiving rAAV2/2 α+β was extended by 67% when compared with mice receiving either rAAV2/2 α or no treatment, ($P < 0.001$; Table 2, which is published as supporting information on the PNAS web site). The effect of β-hexosaminidase expression on the rescue of neurones and its translation into motor function was particularly evident in a subgroup of these mice. Although bilateral movement of the limbs was maintained initially, in the later stages of disease, movement of the right limbs deteriorated in approximately one-third of the animals and resembled that of untreated mice, whereas normal motor function in the left hind and fore limbs was preserved (Movie 2, which is published as supporting information on the PNAS web site). Unilateral preservation of motor function correlated with high expression of β-hexosaminidase activity in the right sensorimotor cortex, left pyramidal tract, and gray matter, as revealed histochemically (Fig. 1). In this subset of mice, on account of the pyramidal decussation, low cortical expression of enzyme activity contralateral to the injection ultimately appeared to be incapable of

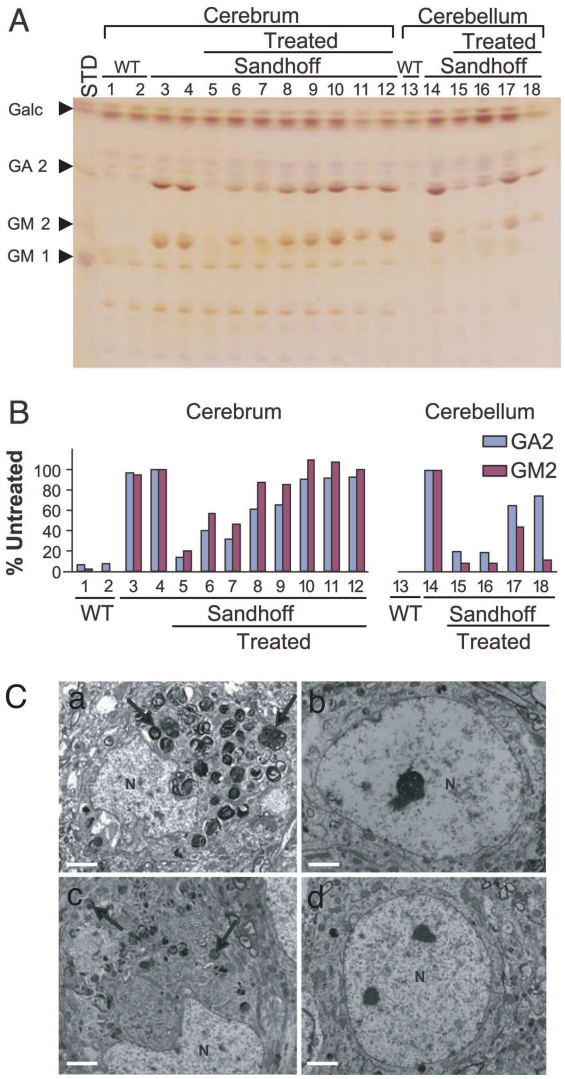

Fig. 2. Quantification and visualization of glycosphingolipids stored in mouse brain. Glycosphinglolipids (GSLs) in untransduced and transduced Sandhoff mouse brain were analyzed by high-performance thin-layer chromatography (*A* and *B*) and electron microscopy (*C*). (*A*) GSLs were extracted from a wild type aged 21 weeks (lanes 1, 2, and 13), an untransduced Sandhoff mouse aged 16 weeks (lanes 3, 4 and 14), or the brains of Sandhoff mice transduced with rAAV$\alpha+\beta$ at a single site in the right striatum (lanes 5–12 and 14–18). Vector was injected at 4 weeks of age; the animals were killed at 16 (lanes 5, 6, and15), 20 (lanes 7, 8, and 16), 24 (lanes 9, 10, and 17), and 30 weeks of age (lanes 11, 12, and 18). Right (lanes 1, 3, 5, 7, 9, and 11) and left cerebrum (lanes 2, 4, 6, 8, 10, and 12) and cerebella (lanes 13–18) were dissected and individually analyzed. Pure GM1, GM2, and GA2 gangliosides and the myelin component, galactocerebroside (Galc), were used as standards (STD). (*B*) GA2 and GM2 content was quantified densitometrically and is represented as the percentage of the content in the untreated Sandhoff mouse, after correcting for loading differences, by using the internal Galc standard. Storage was diminished in all treated Sandhoff brains but increased progressively with age. (*C*) Neuronal ultrastructure in brain sections from wild-type (*d*), untransduced (*c*), and singly rAAV$\alpha+\beta$-transduced Sandhoff mice (*a* and *b*). A single striatal injection of viral vector was given at 4 weeks, and the tissue harvested at 16 weeks of age. Neurons in the transduced ipsilateral cerebral cortex had no membranous cytoplasmic cell bodies (*b*), whereas those in the contralateral cortex (*a*) were distended by the storage vesicles (arrowheads in *a*) with distortion of the nuclei, as in untreated Sandhoff animals (*c*). N, nucleus. (Scale bar: 2 μm.)

sustaining motor function in the corresponding limbs for the entire period of survival.

To improve therapeutic outcomes, multiple injections of vector were tested in seven animals. Sandhoff mice were injected with either rAAV2/2β or rAAV2/1β at four sites, one in each cerebral hemisphere and two in the cerebellum. Each serotype had similar effects. Outcomes could be subdivided into two subgroups: In three mice there was a modest improvement in disease-onset and survival to 151 $\pm$ 10 and 168 $\pm$ 5 days, respectively. However, in four mice, onset of neurological signs was delayed to 265 $\pm$ 23 days and survival was >300 days, with three animals surviving for >1 year (Movie 3, which is published as supporting information on the PNAS web site) and one reaching the humane endpoint only after 312 days. Head tremor never was detected in these animals, but bradykinesia, ataxia, and impaired motor function eventually appeared. Within the entire long-term effect group, the mean onset of neurological signs was delayed by >175% and survival to the endpoint increased by >150%. Mean survival in this subgroup was prolonged by >50%, and disease onset was delayed significantly (>40%) when compared with animals receiving a single therapeutic injection ($P < 0.01$).

To establish whether the sex of the recipients influenced therapeutic outcome, we transduced four males and four females with the rAAV 2/2$\alpha+\beta$ vector. There was no apparent difference in time to the humane endpoint between the sexes of untreated Sandhoff mice or those receiving the control vector, rAAVα (120 $\pm$ 6 and 121 $\pm$ 6 days for males and females, respectively), or between the onset of disease (101 $\pm$ 6 for males and 92 $\pm$ 11 days in female mice). Animals receiving the rAAV 2/2 $\alpha+\beta$ vector showed salutary effects, which appeared to be greater in males with the onset of signs at 221 $\pm$ 30 days compared with 175 $\pm$ 5 for females ($P < 0.03$); times to reach the endpoint were respectively, 253 $\pm$ 40 and 191 $\pm$ 9 days, ($P < 0.03$). Table 3, which is published as supporting information on the PNAS web site, summarizes survival data from the interventions.

Mice in the latter stages of illness lost weight until the predefined humane endpoint was reached; weight loss in Sandhoff mice after gene therapy was markedly delayed, reflecting maintenance of well-being, foraging, and feeding activity (Fig. 4*A*). Motor function, balance, and coordination were assessed by determining the frequency of hind-limb movements during the first 17 weeks (120 days) of life. Distinct performance behaviors were observed in Sandhoff compared with healthy heterozygous and wild-type animals: Unlike the other groups, the frequency of hind-limb movements declined in Sandhoff mice ($P < 0.0001$). Gene therapy prevented this deterioration so that the pattern of hind-limb movements of Sandhoff mice was restored to that observed in wild-type animals (Fig. 4*B*). Horizontal bar and inverted screen tests also were used to evaluate neurological function, which varies with age. The deteriorating performance in these tests by untreated Sandhoff mice (5) also was ameliorated in mice receiving gene therapy (data not shown).

Discussion

Gene therapy delivered to the brain of adult mice has striking effects in an acute knockout model of Tay-Sachs disease, a devastating neurodegenerative disorder. Our findings immediately suggest a role for gene therapy in the glycosphingolipidoses with neurological manifestations and specifically for adeno-associated viral vectors, which have been reported to improve outcomes in animal models of glycoprotein or glycosaminoglycan storage (13, 14).

Treated Sandhoff mice survived uniquely beyond 1 year of age; onset of disease was delayed in animals receiving four inoculations to a mean of 304 days. Gene therapy induced supranormal activities of β-hexosaminidase with widespread and long-lasting expression throughout the brain and spinal cord; neurological improvement was accompanied by reduced ganglioside storage and inflammatory response. Previously, the longest survival, 280 days, was achieved in a subset of mice given a substrate inhibitor combined with bone marrow transplantation (15). Our survival data may underestimate the benefit of rAAV gene therapy because the weight loss end point

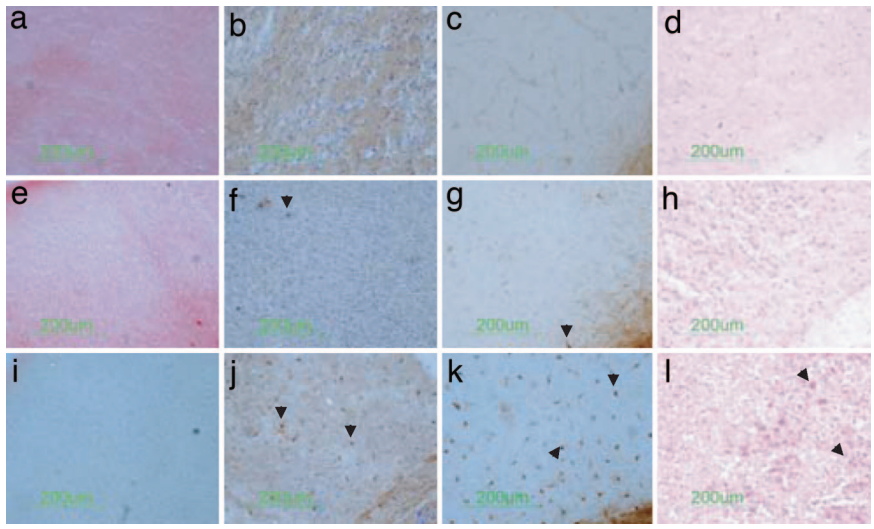

Fig. 3. Relationship between β-hexosaminidase activity, glycosphingolipid storage, and inflammatory cells in the cerebral cortex. Coronal sections from wild type aged 16 weeks (*a–d*), rAAV2/2α+β-transduced aged 29 weeks (humane end point) (*e–h*), and untransduced Sandhoff mice aged 17 weeks (*i–l*) were prepared consecutively. Virus was injected at 4 weeks of age. The β-hexosaminidase reaction product stains red (*a* and *e*) and is absent in untransduced Sandhoff mice (*i*).Glycospingolipid storage, detected by neuronal PAS staining, occurs particularly in layers IV and V of the cerebral cortex of untreated Sandhoff mice (arrowheads in *l*) but was undetectable in cortex from wild-type (*d*) or transduced Sandhoff mice (*h*). Activated microglia/macrophages were recognized by immunostaining of the cell-specific marker, CD68 (*b*, *f*, and *j*), and by binding to isolectin B4 (*c*, *g*, and *k*). No cells of microglia/macrophage lineage were detected in wild-type cortex (*b* and *c*), and only a few were seen in transduced Sandhoff mice (arrowheads in *f* and *g*). Cerebral cortex from untransduced Sandhoff mice contained numerous activated microglia and macrophages (arrowheads in *j* and *k*). The number of neurons staining with PAS and the presence of cells recognized by *G. simplicifolia* isolectin B_4 ($GSIB_4$) and CD68 antibodies inversely depended on enzymatic activity.

used in our studies was chosen earlier in the course of the disease. After gene therapy, Sandhoff mice continued to right themselves after displacement, but loss of this ability was used to define end points for substrate reduction therapy and marrow transplantation; however, onset of tremor was not delayed by the substrate inhibitor (5, 16).

Correction of this inborn error requires global restoration of Hex A and B function, preferably to activities in the range of asymptomatic heterozygotes. Gene delivery by using rAAV meets this need in nonmitotic neural cells: High-titer vectors induce abundant and prolonged expression of β-hexosaminidase without overt cytotoxicity. Strategies were deployed to optimize the outcome of gene therapy based on rAAV, including those to enhance expression and biodistribution (use of the composite pan-neuronal promoter CAGp, which combines the human cytomegalovirus immediate-early enhancer and a modified chicken β-actin promoter and first intron, woodchuck hepatitis virus posttranscriptional regulatory element, and insertion of HIV 1 tat protein transduction domain) as well as AAV serotypes 1 and 2, which almost exclusively infect neurones in the brain and spinal cord (17–20). We also used hyperosmolar mannitol locally to enhance transduction at the injection site (21, 22).

Our rAAV vectors transduce neurones and promote secretion of active β-hexosaminidase for recapture and therapeutic correction at distant sites in the neuraxis. Here we provide evidence of widespread delivery of therapeutic protein to the brain and spinal cord after a single striatal injection with striking restitution of β-hexosaminidase in the transduced striatum and sensorimotor cortex. Appearance of β-hexosaminidase in the pyramidal tract and gray matter of the spinal cord may be explained by anterograde axonal transport of enzyme from transduced cortex, but the heavily stained neuronal cell bodies in the contralateral cortex and substantia nigra argue for retrograde axonal transport from the striatum, either by direct viral transduction or by enzyme uptake. Recent studies using AAV2 vectors favor the latter mechanism (23). We also detected cells expressing β-hexosaminidase within particular laminae of the olfactory bulb, to which they have likely migrated from the strongly staining subventricular zone in the rostral migratory stream, a developmental process that persists in adult brain (23). AAV1, but not AAV2, has been reported to infect ependymal cells (19), yet we found abundant ependymal enzyme activity induced by AAV2 in the ventricles and central canal. The uniformity and extent of ependymal expression renders it likely that the hexosaminidase originates from distant sites and is taken up from cerebrospinal fluid.

In Sandhoff disease, expression of the human β subunit was sufficient to achieve the therapeutic effect and, thus, may dimerize with the endogenous murine α subunit to form hexosaminidase A. Murine sialidase in concert with hexosaminidase B offers a default pathway for GM2 breakdown in mice (4) and might explain the spectacular therapeutic effects of complementation with the β subunit alone. However, the apparent activity ratio of the A to B Hex isozymes in the cerebral hemispheres of Sandhoff mice ipsilateral to the site of rAAV2/2β administration was similar to that in wild-type brain, and cotransfection of α and β subunits enhanced neither this activity ratio nor the therapeutic effect. Although Hex B readily degrades GA2, clearance of this ganglioside was similar that of GM2, as would be predicted in the presence of Hex A.

Expression of β-hexosaminidase in Sandhoff mice reduces ganglioside storage, and storage reduction is correlated with enzymatic activity. Progressive storage with advancing age occurs principally in neural cells without adequate Hex A. Clearance of gangliosides has been reported in the viscera but not in the brain of Sandhoff mice after bone marrow transplantation (24). Delayed storage of brain gangliosides occurs after administration of imino sugars to inhibit glycosphingolipid biosynthesis (5); by the time of death, gangliosides had increased to concentrations observed in the brains of untreated Sandhoff mice. Substrate inhibition, combined with bone marrow transplantation, had a synergistic effect on survival but no additional effect on GA2 storage; indeed, GM2 content was 30% greater than in untreated mice (15). The content of gangliosides in the brains of mice killed at 16–18 weeks that had received gene therapy was greatly diminished when compared with untreated mutant animals of a similar age. Although, with time, after single injections of gene therapy ganglioside content appeared to increase when determined biochemically in regional brain extracts, storage was absent at sites of gene expression when judged histochemically. Widespread clearance of gangliosides judged by both methods was more apparent at the humane endpoint after transduction at several sites. In common with substrate reduction (25) and bone marrow transplantation (9), gene therapy persistently suppressed activation and expansion of microglial and macrophage populations. It is unclear from the timing of previously reported experiments whether substrate reduction or transplantation also led to lifelong suppression of inflammation.

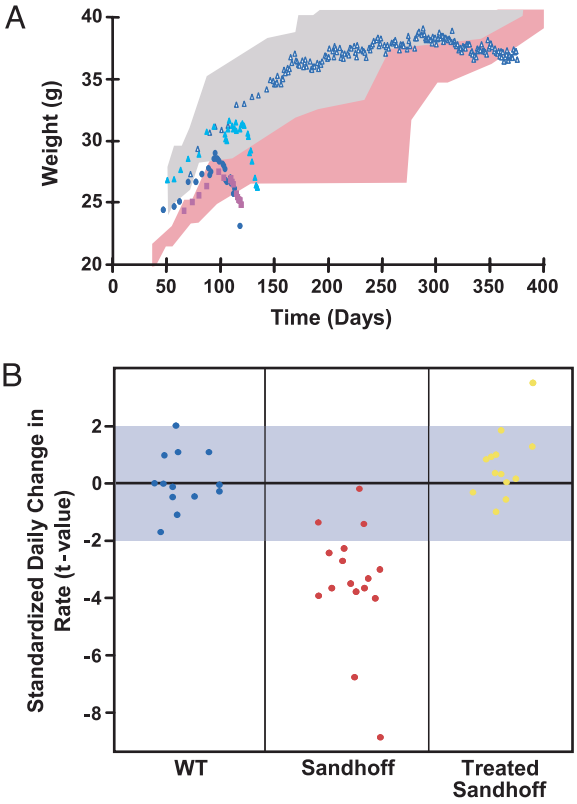

Fig. 4. Survival, weight, and neurological function after gene therapy in Sandhoff mice. Weight and rescue of neurological function was assessed in wild-type, untransduced, and transduced Sandhoff mice. Transduced animals were injected at 4 weeks of age. (*A*) Range of body weights in wild-type mice [blue-gray and pink stippled area for males ($n = 6$) and females ($n = 7$), respectively], untransduced (cyan triangles; $n = 1$) and rAAVα-transduced (dark blue squares; $n = 1$) Sandhoff males, untransduced (pink squares; $n = 5$) Sandhoff females, and rAAV2/2β or rAAV2/1β-transduced Sandhoff males at four sites (open dark blue triangles; $n = 3$). After therapy, Sandhoff mice gained and maintained their weight normally. (*B*) Effect of therapy on hind-limb movements in WT, untransduced or rAAVα-transduced Sandhoff animals (Sandhoff), and Sandhoff mice after transduction with either rAAV2/2β, rAAV2/1β, or rAAV2/2$\alpha+\beta$ (Treated Sandhoff). Each dot represents a single animal. Over 120 days, movement frequency declined in Sandhoff mice ($P = 0.0108$) but, in treated Sandhoff animals, remained indistinguishable from WT ($P = 0.1107$); limb movements improved significantly after gene therapy ($P < 0.0001$).

Gene therapy by using this rAAV vector system delivered intracerebrally to Sandhoff mice with deficient Hex A and B improves the course of acute experimental GM2 gangliosidosis. Ultimate deterioration, despite high β-hexosaminidase activities with reduced ganglioside storage and inflammation, remains unexplained; it may result from visceral or lethal neurological disease beyond the reach of stereotaxic gene therapy. Late development of immune reactions is unlikely, because hexosaminidase function persisted. Further studies combining brain and early peripheral gene therapy, or the adjunctive use of substrate inhibitors and/or bone marrow transplantation, will address these issues. We predict that combined modalities would show at least an additive therapeutic effect. Given the availability of iminosugars for therapeutic use in glycosphingolipidoses (26, 27), transduction of human β-hexosaminidase by using rAAV vector constructs based on those described here, is a promising combinatorial strategy for clinical application in human Tay-Sachs-related diseases.

Materials and Methods

Experimental Animals. The Sandhoff disease mouse (strain: B6; 129S-Hexb^{tm1Rlp}) model developed by disruption of the hexb gene (4) was obtained from The Jackson Laboratory. The strain was maintained by crossing homozygous males with heterozygous females or by heterozygous matings. These studies were conducted by using protocols approved under license by the U.K. Home Office (Animals Scientific Procedures Act, 1986). The hexb genotype was determined by PCR on mouse-tail DNA with primers B3: (5′-ATGTGGATGCAACTAACC-3′) and B4 (5′-AGGTTGTG-CAGCTATTCC-3′) that flank the disrupting MC1NeopolyA cassette in exon 13. Symptomatic homozygous Sandhoff mice received nutritional supplements (Transgel; Charles River Laboratories). The approved humane end point, applied to mice throughout these studies, was defined as the loss of between 9% and 10% of presymptomatic body weight.

Vector Construction and Production. The AAV2 plasmid vector used for the production of rAAV2/2α, rAAV2/1α, rAAV2/2β, and rAAV2/1β was generated by subcloning the expression cassettes encoding human β-hexosaminidase α and β subunits into pAAVSP70, a derivative of pAV1 (28). To generate the expression cassettes hexα and hexβ, cDNAs were synthesized by RT-PCR (Stratagene) by using total RNA isolated from human liver as a template and cloned into the plasmid pcDNA3 (Invitrogen). Primers A3 (5′-TTGGTGGAGAGGCTTG-TATG-3′) and Atat (5′-TGCTCTAGAAATCATCTTCG-TCGCTGTCTCCGCTTCTTCC TGCCATAACCGCCAC-CGCCGGTCTGTTCAAACTCCTGCTCACA-3′); B3 (5′-ATGTGGATGCAACTAACC-3′) and Btat (5′-TGCTCTA-GTCATCTTCGTCG CTGTCTCCGCTTCTTCCTGC CATA-ACCGCCACCGCCCATGTTCTCATGGTTACAATATCC-3′) were used to engineer the hexα-HIVtat and hexβ-HIVtat fusion proteins, respectively. PCR products were digested with HincII/XbaI and PstI/XbaI, respectively, and cloned into similarly cut vectors containing hexα and hexβ cDNAs. The woodchuck hepatitis virus posttranscriptional regulatory element (WPRE) was amplified by PCR from viral genomic DNA (American Type Culture Collection, Middlesex, U.K.) with primers WPRE1 (5′-GCGGATCCTGTTAATCAACCT-CTGG-3′) and WPRE2 (5′-TAGGG CCCTGAAGACCAAG-CAACAC-3′) and cloned downstream of the hexα and hexβ fusion cDNAs. The bovine growth hormone polyadenylation signal sequence (BGHpA) was that of plasmid pcDNA3. The composite promoter CAG was cut from plasmid pDRIVE-CAG (InvivoGen, San Diego) and cloned into plasmid pAAVSP70 upstream of the transcriptional cassettes.

Recombinant AAV viruses were produced by triple plasmid cotransfection of HEK 293 cells by using pAAVSP70 harboring the expression cassettes, an adenovirus helper plasmid, and a chimeric packaging construct expressing the AAV2 rep gene and either the AAV2 or AAV1 cap genes. rAAV2/2 viruses were purified by affinity column chromatography (29) (produced at the University of Pennsylvania Vector Core Facility, Philadelphia). rAAV2/1 viruses were purified by ion-exchange chromatography (ref. 30; produced at Genzyme Corp.). DNase-resistant viral genome copies (drps) of the AAV vectors were determined by using a real-time TaqMan PCR assay (ABI Prism 7700; Applied Biosystems, Foster City, CA) with primers specific for the BGHpA sequence. The titers were 2.9×10^{12}, 7.1×10^{12}, 5.5×10^{12}, and 4.9×10^{12} drps/ml for rAAV2/2α, rAAV2/2β, rAAV2/1α, and rAAV2/1β, respectively.

Intracranial Stereotaxic Inoculation of rAAV Vectors. Four-week-old Hexb$-/-$ Sandhoff mice were anaesthetized and placed in a stereotaxic frame (Kopf Instruments, Tujunga, CA). Burr holes were drilled over target sites, and vector mix was delivered vertically by using coordinates relative to bregma and dura. Single-site injections into the striatum were at: anterior posterior (AP), -0.1 mm; medial-lateral (ML), -2.0 mm; and dorsal-ventral (DV) -3.0 mm. For injections at four sites, two were delivered into the striatum, AP, -0.1 mm; ML, ± 2.0 mm; and DV, -3.0 mm, and two

into the cerebellum, AP, −6.0 mm; ML, ±1.5 mm; DV, −3.0 mm. Animals received 3 μl of vector mix for single injections and 2.5 μl per site for four-site injections (total 10 μl). We used a volume ratio of 1.1:1.1:0.8 (rAAVα:rAAVβ:20% mannitol) for rAAVα+β injections. When injecting rAAVα or rAAVβ alone, the ratio was 2.2:0.8 (rAAV: 20% mannitol). The infusion rate was 0.8 μl/min. The needle was withdrawn after 5 min. After giving postoperative analgesia (Rimadyl, Large Animal Solution; Pfizer, Kent, U.K.), the mice were placed in an incubator at 37°C to recover.

Tissue Processing and Staining. Mice were fixed by intracardiac perfusion with paraformaldehyde. Sections (45 μm) were exposed to rat anti-mouse CD68 (Serotec, Oxford,) and *G. simplicifolia* isolectin B_4 (biotinylated, α-D-galactosyl-specific, Vector Laboratories, Peterborough, U.K.). Staining was based on the avidin-biotin peroxidase technique (31). Biotinylated rabbit anti-rat IgG secondary antibody (Vector Laboratories) and isolectin were detected by using Vectastain (Vector Laboratories) and developed with 3,3′-diaminobenzidine with Cresyl violet as counterstain. β-hexosaminidase activity was detected with naphthol AS-BI *N*-acetyl-β-glucosaminide (Sigma, Poole Dorset, U.K.) (32). PAS staining (Sigma) was followed by counterstaining with haematoxylin. Sections were mounted in dibutyl phthalate xylene (BDH).

For electron microscopy, perfuse-fixation with 50 ml intracardiac PBS (pH 7.4) containing 0.05% sodium nitrite was followed by 100 ml of 1% paraformaldehyde/3% glutaraldehyde in 0.1 M Pipes (pH 7.4) with 4 h after fixation at 4°C; after several washes in buffer, tissues were treated with 1% osmium ferricyanide for 1 h at 4°C and stained with 1% uranyl acetate and lead citrate. Thin sections were examined after dehydration and embedding.

Assays of β-hexosaminidase and gangliosides used tissues from mice killed by asphyxiation. Tissue extracts in 0.01 M phosphate-citrate buffer (pH 4.4) were assayed fluorimetrically for β-hexosaminidases with 4-methylumbelliferyl-β-*N*-acetylglucosaminide as substrate (Sigma). HEXA was calculated as the difference between total β-hexosaminidase (before) and HEXB activity (after) heat inactivation (12). Fluorescence was determined in a PerkinElmer LS30 fluorimeter. Protein was quantified by the Pierce protein assay (MicroBCA Reagent).

For glycosphingolipid analysis, lyophilised aqueous tissue homogenates were extracted with chloroform: methanol (2:1), dried under nitrogen and after redissolving in solvent, extracts equivalent to 250–500 μg of dried tissue were separated alongside pure standards by high-performance thin-layer chromatography (silica gel 60, Merck) in chloroform:methanol:0.22% $CaCl_2$ (60:35:8, vol/vol). Dried plates were sprayed with orcinol:sulfuric acid and baked at ≈90°C for 15 min. The intensity of individually resolved species was quantified by densitometry by using NIH IMAGEJ software employing galactocerebroside present in each extract to correct for loading differences.

Neurological Evaluation. Tremor and bradykinesia were evaluated by inspection of mutant, compared with wild-type or heterozygous mice, after removal from their cages to a flat surface.

Horizontal bar and inverted screen tests were used between 0900 and 1800 hours to score combined motor coordination, balance, and limb strength, which vary with time and in response to interventions (5). In the inverted screen test, the mouse was positioned in the center of a metal mesh and slowly inverted. Latency of falling from the screen over a padded surface, as well as the number of times the hind paws released and grasped the mesh, was recorded within 2 min (5).

Statistical Analyses. Unless stated, data are expressed as means with SD; comparisons between groups were evaluated by the Mann–Whitney test. To avoid bias due to differences in survival between treated and untreated mice, the effect of gene therapy on hind-limb movement was considered only during the first 120 days of life. For each observation, the frequency of hind-limb movement was calculated, and a linear model fitted to the observations from each animal to detect any trends in that frequency with time. The linear model was weighted by observation time to account for the increased confidence in some estimates of the frequency. The linear coefficients from the models then were compared graphically; proportions with increasing or decreasing trends were compared by Fisher's exact test.

We thank Philip Ball for the artwork, Mark Bartley and Steve Atherton for movie recordings, Dr. M. Jeyakumar for advice on lipid analysis, and Janet Powell (Wellcome Trust Imaging Center, Cambridge, U.K.) for processing tissues for electron microscopy. Trevor Richards kindly facilitated the conduct of this work and Dr. Donald Harter provided warm support and encouragement. This work was supported by a generous gift from The Paul Morgan Trust, an unrestricted grant from Cambridge in America, and a grant from National Health Service Executive Eastern.

1. Gravel, R. A., Kaback, M. M., Proia, R. L., Sandhoff, K., Suzuki, K. & Suzuki, K. (2001) in *The Metabolic and Molecular Bases of Inherited Disease*, eds. Scriver, C. R., Beaudet, A. L., Sly, W. S. & Valle, D. (McGraw–Hill, New York), 8th Ed., Vol. 3, pp. 3827–3876.
2. Cork, L. C., Munnell, J. F., Lorenz, M. D., Murphy, J. V., Baker, H. J. & Rattazzi, M. C. (1977) *Science* **196,** 1014–1017.
3. Fox, J., Li, Y. T. & Dawson, G. (1999) *Acta Neuropathol.* **97,** 57–62.
4. Sango, K., Yamanaka, S., Hoffmann, A., Okuda, Y., Grinberg, A., Westphal, H., McDonald, M. P., Crawley, J. N., Sandhoff, K., Suzuki, K. & Proia, R. L. (1995) *Nat. Genet.* **11,** 170–176.
5. Jeyakumar, M., Butters, T. D., Cortina-Borja, M., Hunnam, V., Proia, R. L., Perry, V. H., Dwek, R. A. & Platt, F. M. (1999) *Proc. Natl. Acad. Sci. USA* **96,** 6388–6393.
6. Walkley, S. U., Baker, H. J., Rattazzi, M. C., Haskins, M. E. & Wu, J. Y. (1991) *J. Neurol. Sci.* **104,** 1–8.
7. Neuenhofer, S., Conzelmann, E., Schwarzmann, G., Egge, H. & Sandhoff, K. (1986) *Biol. Chem. Hoppe-Seyler* **367,** 241–244.
8. Zhou, D., Mattner, J., Cantu, C., III, Schrantz, N., Yin, N., Gao, Y., Sagiv, Y., Hudspeth, K., Wu, Y. P., Yamashita, T., *et al.* (2004) *Science* **306,** 1786–1789.
9. Wada, R., Tifft, C. J. & Proia, R. (2000) *Proc. Natl. Acad. Sci. USA* **97,** 10954–10959.
10. Wu, Y.-P. & Proia, R. L. (2004) *Proc. Natl. Acad. Sci. USA* **101,** 8425–8430.
11. Yamaguchi, A., Katsuyama, K., Nagahama, K., Takai, T., Aoki, I. & Yamanaka, S. (2004) *J. Clin. Invest.* **113,** 200–208.
12. Shapira, E., Blitzer, M. G., Miller, J. B. & Africk, D. K. (1989) in *Biochemical Genetics, A Laboratory Manual* (Oxford Univ. Press, New York).
13. Vite, C. H., McGowan, J. C., Niogi, S. N., Passini, M. A., Drobatz, K. J., Haskins, M. E. & Wolfe, J. H. (2005) *Ann. Neurol.* **57,** 355–364.
14. Liu, G., Martins, I., Wemmie, J. A., Chiorini, J. A. & Davidson, B. L. (2005) *J. Neurosci.* **25,** 9321–9327.
15. Jeyakumar, M., Norflus, F., Tifft, C. J., Cortina-Borja, M., Butters, T. D., Proia, R. L., Perry, V. H. & Platt, F. M. (2001) *Blood* **97,** 327–329.
16. Andersson, U., Smith, D., Jeyakumar, M., Butters, T. D., Borja, M. C., Dweek, R. A. & Platt, F. M. (2004) *Neurobiol. Dis.* **16**, 506–515.
17. Xia, H., Mao, Q. & Davidson, B. L. (2001) *Nat. Biotechnol.* **19,** 640–644.
18. Zufferey, R., Donello, J. E., Trono, D. & Hope, T. J. (1999) *J. Virol.* **73,** 2886–2892.
19. Passini, M. A., Watson, D. J., Vite, C. H., Landsburg, D. J., Feigenbaum, A. L. & Wolfe, J. H. (2003) *J. Virol.* **77,** 7034–7040.
20. Burger, C., Gorbatyuk, O. S., Velardo, M. J., Peden C. S., Williams. P., Zolotukhin, S., Reier, P. J., Mandel, R. J. & Muzyczka, N. (2004) *Mol. Therapy* **10,** 302–317.
21. Bourgoin, C., Emiliani, C., Kremer, E. J., Gelot, A., Tancini, B., Gravel, R. A., Drugan, C., Orlacchio, A., Poenaru, L. & Caillaud, C. (2003) *Gene Ther.* **10,** 1841–1849.
22. Burger, C., Nguyen, F. N., Deng, J. & Mandel, R. J. (2005) *Mol. Ther.* **11,** 327–331.
23. Passini, M. A., Lee, E. B., Heuer, G. G. & Wolfe J. H. (2002) *J. Neurosci.* **22,** 6437–6446.
24. Norflus, F., Tifft, C. J., McDonald, M. P., Goldstein, G., Crawley, J. N., Hoffmann, A., Sandhoff, K., Suzuki, K. & Proia, L. (1998) *J. Clin. Invest.* **101,** 1881–1888.
25. Jeyakumar, M., Thomas, R., Elliot-Smith, E., Smith, D. A., van der Spoel, A. C., d'Azzo, A., Perry, V. H., Butters, T. D., Dwek, R. A. & Platt, F. M. (2003) *Brain* **126,** 974–987.
26. Cox, T. M., Aerts, J. M., Andria, G., Beck, M., Belmatoug, N., Bembi, B., Chertkoff, R., Vom Dahl, S., Elstein, D., Erikson, A., *et al.* (2003) *J. Inherit. Metab. Dis.* **26,** 513–526.
27. Lachmann, R. H., te Vruchte, D., Lloyd-Evans, E., Reinkensmeier, G., Sillence, D. J., Fernandez-Guillen, L., Dwek, R. A., Butters, T. D., Cox, T. M. & Platt, F. M. (2004) *Neurobiol. Dis.* **16,** 654–658.
28. Laughlin, C. A., Tratschin, J. D., Coon, H. & Carterm, B. J. (1983) *Gene* **23,** 65–73.
29. Auricchio, A., Hildinger, M., O'Connor, E., Gao, G. P. & Wilson, J. M. (2001) *Hum. Gene Ther.* **12,** 71–76.
30. O'Riordan, C. R., LaChapelle, A. L., Vincent, K. A. & Wadsworth, S. C. (2000) *J. Gene Med.* **2,** 444–454.
31. Hsu, S. M., Raine, L. & Fanger, H. (1981) *J. Histochem. Cytochem.* **29,** 577–580.
32. Lacorazza, H. D. & Jendoubi, M. (1995) *BioTechniques* **19,** 434–439.